

1 **Urinary Astrocyte-derived Extracellular Vesicles: A Non-invasive Tool for Capturing**

2 **Human *In Vivo* Molecular “Movies” of Brain**

3

4 Xin-hui Xie<sup>1†\*</sup>; Mian-mian Chen<sup>1†</sup>; Shu-xian Xu<sup>1</sup>; Jun-hua Mei<sup>1,3</sup>; Qing Yang<sup>3</sup>; Chao Wang<sup>1</sup>;

5 Zhongchun Liu<sup>1,2\*</sup>

6

7 Affiliations:

8 1. Department of Psychiatry, Renmin Hospital of Wuhan University, Wuhan, Hubei, PR

9 China.

10 2. Taikang center for life and medical sciences, Wuhan University, Wuhan, PR China.

11 3. Department of Neurology, Wuhan First Hospital, Wuhan, Hubei, PR China.

12

13

14 †These authors have contributed equally to this work.

15

16 \*Corresponding author:

17 Xin-hui Xie.

18 Address: 1) Department of Psychiatry, Renmin Hospital of Wuhan University, No. 99 Jiefang

19 Road, Wuchang District, Wuhan, Hubei, PR China. ZIP: 430060. Telephone:

20 86-8804191181399.

21 E-mail: xxh.med@gmail.com; xin-hui.xie@live.com

22

23 Zhongchun Liu.

24 Address: 1) Department of Psychiatry, Renmin Hospital of Wuhan University, No. 99 Jiefang

25 Road, Wuchang District, Wuhan, Hubei, PR China. ZIP: 430060. Telephone:

26 86-8804191181399. 2) Taikang center for life and medical sciences, Wuhan University,

27 Wuhan, PR China. ZIP: 430071.

28 E-mail: zcliu6@whu.edu.cn

29

30

31

### 32 **Author Contributions.**

33 Xin-hui Xie: Conceptualization, Methodology, Formal analysis, Investigation, Writing -

34 Original Draft, Writing - Review & Editing, Visualization, Supervision. Mian-mian Chen:

35 Investigation, Methodology, Writing - Original Draft. Shu-xian Xu: Methodology,

36 Investigation, Writing - Original Draft. Jun-hua Mei: Investigation, Writing - Original Draft.

37 Qing Yang: Investigation, Writing - Original Draft. Chao Wang: Methodology, Writing -

38 Review & Editing. Zhongchun Liu: Funding Acquisition, Project Administration,

39 Supervision.

40

### 41 **Conflict of Interest Statement**

42 The authors declare they have no conflict of interest.

43

### 44 **Acknowledgement**

45 This work was supported by grant from the National Natural Science Foundation of China  
46 (grant number: U21A20364). This work has not received funding/assistance from any  
47 commercial organizations. The funding source had no roles in the design of this study and  
48 will not have any roles during the execution, analyses, interpretation of the data, or decision  
49 to submit results.

50

51

52 Number of words in abstract: 245

53 Number of words in main text: 4109

54

55 **Abstract**

56 The identification of particularly individual-level biomarkers, for certain central nervous  
57 system (CNS) diseases remains challenging. A recent approach involving the enrichment of  
58 brain-derived extracellular vesicles (BDEVs) from peripheral blood has emerged as a  
59 promising method to obtain direct *in vivo* CNS data, bypassing the blood-brain barrier.  
60 However, for rapidly evolving CNS diseases (*e.g.*, weeks or even days), the Nyquist-Shannon  
61 sampling theorem dictates the need for a high-frequency sampling rate. Obviously, daily  
62 collection of blood or cerebrospinal fluid from human subjects is impractical. Thus, we  
63 innovated a novel method to isolate astrocyte-derived EVs from urine (uADEVs). It involves  
64 three main steps: 1) concentrating urine samples, 2) isolating total EVs from urine (uTEVs)  
65 using ultracentrifugation, and 3) using an anti-glutamate/aspartate transporter (GLAST)  
66 antibody to isolate GLAST<sup>+</sup>EVs from uTEVs. Subsequently, we confirmed the identity of  
67 these GLAST<sup>+</sup>EVs as uADEVs using transmission electron microscopy, nanoparticle tracking  
68 analysis, western blotting, and the measurement of astrocyte-related neurotrophins.  
69 Furthermore, we applied the uADEVs protocol to depict the detailed trajectory of the  
70 N-methyl-d-aspartic acid receptor (NMDAR) subunit zeta-1 (GluN1) in an anti-NMDAR  
71 encephalitis patient, demonstrated the potential of this method for capturing intricate  
72 trajectories of CNS-specific molecular *in vivo* signals at the individual level. This  
73 non-invasive approach enables frequent sampling, up to daily or even half-daily, analogous to  
74 capturing molecular “movies” of the brain, coupled with appropriate signal processing  
75 algorithms, holds promise for identifying novel biomarkers or illuminating the etiology of  
76 rapidly evolving CNS diseases by tracking the precise trajectories of target molecules.

77

78

79 **Keywords:** urinary astrocyte-derived extracellular vesicles; human *in vivo*; non-invasive;

80 central nervous system; high-frequent sampling; anti-N-methyl-d-aspartic acid receptor

81 encephalitis; biomarker; wavelet analysis

## 82 **Introduction**

83 Research on central nervous system (CNS) diseases, especially mental disorders like  
84 schizophrenia, depression, and bipolar disorder, has been gradual, and reliable biological  
85 markers remain unidentified<sup>1,2</sup>. Several key factors may contribute to this dilemma.

86 To begin, the CNS boasts distinctive attributes, notably the presence of the blood-brain  
87 barrier (BBB), which poses a direct hurdle to identifying CNS abnormalities<sup>3</sup>. This challenge  
88 is compounded by the BBB's high selectivity, leading to marked inconsistencies in the  
89 expression levels of molecules within the CNS compared to the periphery<sup>4-7</sup>. Such  
90 incongruities substantially complicate research endeavors. Additionally, the dearth of  
91 expedient and non-invasive sampling techniques is notable. The most direct sampling method  
92 for the CNS is brain biopsy, but this is clearly very difficult to perform. Another option,  
93 cerebrospinal fluid (CSF) collection via lumbar puncture, is neither unsuitable for routine  
94 application. While peripheral blood is the most commonly employed biological sample, its  
95 representation of the CNS is limited<sup>4,8,9</sup>.

96 Furthermore, a paucity in sampling frequency is evident. Although reliable biomarkers  
97 have been identified for specific neurological and psychiatric disorders like Alzheimer's  
98 disease (AD) and Parkinson's disease (PD)— $A\beta$ <sup>10,11</sup>, tau<sup>12,13</sup>, and  $\alpha$ -synuclein<sup>14</sup>. These  
99 biomarkers greatly expedited research in these domains, but a tacit assumption should not be  
100 ignored: these disorders exhibit protracted disease courses. Adopting a wave-based  
101 perspective, these biomarkers' trajectories resemble long waves, with wavelengths spanning  
102 years or decades. Therefore, according to the Nyquist-Shannon sampling theorem<sup>15</sup>, detecting  
103 these extended biomarker waves necessitates lower frequencies, rendering half-yearly or

104 yearly sampling adequate. However, for disorders characterized by rapid fluctuations—such  
105 as depression, bipolar disorder, encephalitis, and others—exhibiting weekly, daily, or even  
106 hourly changes, routine follow-up intervals (monthly, half-yearly, or yearly) fall short of  
107 capturing the molecular trajectories which aligned with symptom progression. And since daily  
108 sampling of peripheral blood or CSF is impractical, there is a need for a new methodological  
109 approach that can quickly and non-invasively explore the CNS and facilitate research on these  
110 rapidly changing neurological and psychiatric diseases. We focused on extracellular vesicles  
111 (EVs) as a potential tool for this purpose.

112 EVs are found in various bodily fluids, including blood, urine, tears, and saliva<sup>16</sup>, and  
113 have emerged as promising tools for identifying disease biomarkers, serving as liquid  
114 biopsies<sup>17</sup>. Notably, EVs can cross the BBB bidirectionally<sup>18</sup>, making brain-derived EVs  
115 (BDEVs) a potential “window to the brain”<sup>19</sup>. In a large-sample trial, the concentrations of  
116 T-tau, P-T181-Tau, and A $\beta$ <sub>1-42</sub> in serum neuro-derived EVs (NDEVs) were linearly associated  
117 with their concentrations in CSF with correlation coefficients close to 0.9<sup>20</sup>. Furthermore,  
118 these NDEVs were able to predict the onset of AD<sup>21</sup>. Similarly, in the case of PD,  $\alpha$ -synuclein,  
119 a biomarker of PD, was found to be elevated in NDEVs in PD patients<sup>22-26</sup>, and the area under  
120 the receiver operating characteristic curve (ROC) exceeded 0.9<sup>27</sup>. Additionally, animal studies  
121 also shown a high level of consistency between plasma astrocyte-derived EVs (ADEVs) and  
122 brain homogenous (BH)<sup>28</sup>. In short, the plasma/serum BDEVs could be good proxies of  
123 CNS<sup>29,30</sup>. However, the collection of peripheral blood is also an invasive procedure that is  
124 impractical for daily sampling, limiting the sampling rate for obtaining *in vivo* signals from  
125 the CNS using plasma/serum BDEVs. Additionally, the presence of heteroproteins in

126 peripheral blood makes it challenging and inconvenient to isolate EVs from specific cell  
127 sources.

128 To bypass the disadvantages of isolating BDEVs from peripheral blood, we focused on  
129 another type of body fluid—urine, which also contains a large amount of EVs<sup>31</sup>. Urine is an  
130 optimal body fluid for identifying diagnostic biomarkers due to its capacity for large-scale  
131 and high-frequency collection, as well as its non-invasive nature. Urinary EVs (uEVs) have  
132 been implicated in the pathophysiological mechanisms of urogenital diseases and hold  
133 potential as molecular biomarkers for these conditions<sup>32–35</sup>. Initially, uEVs were thought to  
134 originate primarily from cells in the urogenital tract, including the kidneys, bladder, and sex  
135 glands<sup>36</sup>. However, given that primary urine results from plasma filtration in the glomeruli,  
136 EVs in blood might enter and be detected in urine<sup>37,38</sup>. For example, the labeled EVs were  
137 injected intravenously into rats, and later found in their urine<sup>39</sup>. Wang et al. identify neuronal  
138 marker protein in urinary total EVs (uTEVs)<sup>35</sup>, and Fraser et al. reported elevated levels of  
139 ser(P)-1292 LRRK2, a PD-associated protein, in uTEVs of PD patients, correlating with  
140 cognitive and daily function impairments<sup>32</sup>. It suggests a possibility that non-urogenital EVs,  
141 including BDEVs, can enter urine and be isolated. As EVs are considered to reflect the state  
142 of their origin cells, and urine is a readily accessible and non-invasive biofluid, the  
143 successful isolation of specific EVs from urine could therefore serve as a valuable tool for  
144 diagnostic and physiological research.

145 Thus, here we developed a protocol that enables the enrichment of the  
146 glutamate/aspartate transporter (GLAST)<sup>+</sup>EVs which is believed to be ADEVs<sup>40–47</sup> from  
147 urine, namely urinary ADEVs (uADEVs). We believe that uADEVs could serve as a

148 valuable tool for non-invasive, high-frequency daily sampling of human *in vivo* CNS signals,  
149 enabling the collection of large-scale longitudinal data on the dynamic behavior of these  
150 cells.

151 **2. Materials and Methods**

152 This study was conducted at Renmin Hospital of Wuhan University (Mental Health  
153 Center of Hubei Province, Wuhan, Hubei, China) and Wuhan First Hospital in compliance  
154 with the Declaration of Helsinki (revised edition, 2013)<sup>48</sup>. The study protocol was approved  
155 by both the Human Ethics Committee of Renmin Hospital of Wuhan University and Wuhan  
156 First Hospital. All participants provided informed consent and were free to withdraw from the  
157 trial at any time for any reason.

158

159 **2.1 Isolation protocol of uADEVs**

160 Generally, in this protocol, we first concentrated the urine samples and isolated the  
161 uTEVs using ultracentrifugation (UC), followed by the isolation of uADEVs using  
162 biotin-anti-GLAST-antibody, similar to the isolation of ADEVs from plasma or serum<sup>40–47,49</sup>.  
163 The flow chart of this protocol is depicted in **Figure 1(a)**.

164

165 **2.1.1 Isolation of uTEV**

166 Nine healthy volunteers, comprising six males and three females, participated in the  
167 study. The median age of the participants was 25.0 years with an interquartile range (IQR) of  
168 4.0 years. A total of 300–600 ml of fresh morning urine of each participant was collected and  
169 promptly delivered to the laboratory. The samples were processed within two hours of  
170 collection. The urine sample was centrifuged at room temperature (RT) for 30 minutes at  
171 2,000 g, and the supernatant was collected. Subsequently, sodium chloride (NaCl) was added  
172 to a concentration of 0.58 M and incubated at RT for 2 hours to eliminate urinary

173 mucoproteins, including Tamm-Horsfall protein<sup>50,51</sup>. The mixture was then centrifuged again  
174 at RT for 30 minutes at 8,000 g, and the supernatant was collected. The sample was filtered  
175 using a 0.45 µm filter membrane (Millipore, MA, USA, Catalog# HVLP07625), and then  
176 loaded into a concentration device (Amicon® stirred cell, Millipore, MA, USA, Catalog#  
177 UFSC40001) and ultrafiltered to a volume of 3–4 ml using a 10 kDa NMW ultrafiltration (UF)  
178 disc membrane (Millipore, MA, USA, Catalog# PLGC07610). Next, 200 ml of PBS was  
179 added, and the sample was ultrafiltered to a volume of approximately 3–4 ml again, resulting  
180 in a concentrated component. The concentrated component was transferred to an  
181 ultracentrifuge tube and centrifuged at 150,000 g at 4°C for 150 minutes (SW60Ti,  
182 OptimaXE-100, Beckman Coulter, Fullerton, CA). The supernatant was discarded, and the  
183 precipitation was resuspended in 350 µl of Dulbecco's phosphate-buffered saline (DPBS,  
184 Beyotime, Catalog# C0221D) containing protease and phosphatase inhibitors (PPICs,  
185 Beyotime, Catalog# P1046). This resulted in a uTEV sample.

186

### 187 **2.1.2 Isolation of uADEVs**

188 Each uTEV sample was mixed with 50 µl of 3% bovine serum albumin (BSA, Beyotime,  
189 Catalog# ST023-50g) and incubated for 1 hour at RT with 4 µl of anti-GLAST  
190 (ACSA-1)-biotin antibody (Miltenyi Biotec, Catalog# 130-118-984). Subsequently, 10 µl of  
191 streptavidin-agarose resin (Thermo Fisher Scientific, Catalog# 53116) and 40 µl of 3% BSA  
192 were added, followed by incubation for 60 minutes at RT. After centrifugation at 800 g for 10  
193 minutes at 4°C and removal of the supernatant, each sample was resuspended in 100 µl of  
194 cold 0.1M glycine-HCl (pH = 3.0) by gently mixing for 30 seconds. The suspension was then

195 centrifuged at 4,000 g for 10 minutes at 4°C, and the supernatant was collected. Several drops  
196 of 1M Tris-HCl (pH = 8.0, Beyotime, Catalog# ST780-500ml) was added to adjust the pH to  
197 7.0. This resulted in a uGLAST<sup>+</sup>EV sample. For western blotting and protein measurements,  
198 mammalian protein extraction reagent (M-PER, Thermo Fisher Scientific, Catalog# 78503)  
199 with PPICs was added to each uADEV sample or uTEV sample.

200

### 201 **2.1.3 Validation of uADEVs**

#### 202 **2.1.3.1 Transmission electron microscopy (TEM)**

203 Similar to our previous ADEV studies<sup>47,52</sup>, the TEM was used to get the image of EVs.  
204 Twenty µl of the EV sample was added dropwise to 200-mesh grids and incubated at RT for  
205 10 minutes, then the grids were negatively stained with 2% phosphotungstic acid for 3  
206 minutes, and the remaining liquid was removed by filter paper. Then observed with a HT7800  
207 transmission electron microscope (Hitachi High-Tech Corporation, Tokyo, Japan).

208

#### 209 **2.1.3.2 Nanoparticle tracking analysis (NTA)**

210 The diameter (nm) and concentration (particles/ml) of EV samples were determined  
211 using the ZetaView PMX 110 (Particle Metrix, Meerbusch, Germany) with ZetaView 8.04.02  
212 nanoparticle tracking software (Particle Metrix, Meerbusch, Germany).

213

#### 214 **2.1.3.3 Western blotting**

215 Western blot was conducted to detect three EV markers with primary rabbit anti- $\alpha$ cluster  
216 of differentiation (CD)63 antibody (Abcam, Catalog# ab134045), rabbit anti- $\alpha$ CD9 antibody

217 (Abcam, Catalog# ab125011), and mouse anti-Alix antibody (Proteintech, Catalog#  
218 67715-1-Ig), an astrocyte marker with rabbit anti-glial fibrillary acidic protein (GFAP)  
219 antibody (Abcam, Catalog# ab68428), and two kidney markers Na<sup>+</sup>-K<sup>+</sup>-Cl<sup>-</sup> cotransporter  
220 (NKCC) 2 (Abcam, Catalog# ab171747), sodium-chloride cotransporter (NCC) (Abcam,  
221 Catalog# ab95302).

222

#### 223 **2.1.3.4 Protein measurements**

224 Astrocyte related neurotrophins (brain-derived neurotrophic factor (BDNF), epidermal  
225 growth factor (EGF), fibroblast growth factor (FGF)-2, glial cell-derived neurotrophic factor  
226 (GDNF), GFAP, nerve growth factor beta (NGF-β), S100 calcium binding protein B (S100B))  
227 were measured using the Human ProcartaPlex™ Simplex kit (Thermo Fisher Scientific,  
228 Catalog# PPX-07).

229

#### 230 **2.1.4 Statistical methods**

231 For comparisons between uTEVs and uADEVs, the concentrations of neurotrophins  
232 (pg/ml) were normalized to a reference of 10E+10 particles/ml, yielding values in pg/per  
233 10E+10 particles, adhering to MISEV2018<sup>16</sup>. The fold change of the uADEVs/uTEVs ratios  
234 were calculated for both particle and neurotrophin concentrations. Welch's two sample *t*-tests  
235 were employed to test the differences of each parameter between the uADEVs and uTEVs  
236 samples. A two-sided *p*-value <0.05 was considered statistically significant. All statistical  
237 analyses were performed using R version 4.2.0 (R Project for Statistical Computing) within  
238 Rstudio version 1.4.1106 (Rstudio).

239

240 **2.2 Case: the potential ability of uADEVs on depicting the trajectories of target**  
241 **molecules in CNS.**

242 To assess the potential of uADEVs in tracking the trajectories of *in vivo* target molecules  
243 in the CNS, we analyzed CSF, uADEV, and blood samples from a middle-aged female patient  
244 (Patient A) with anti-N-methyl-d-aspartic acid receptor (NMDAR) encephalitis probably  
245 caused by teratoma. N-methyl-d-aspartic acid receptor (NMDAR) subunit zeta-1 (GluN1), the  
246 pathogenic molecule in anti-NMDAR encephalitis, was measured in CSF and uADEV  
247 samples using the enzyme-linked immunosorbent assay (ELISA) (CUSABIO, Catalog#  
248 CSB-EL009911HU). Given the patient's comatose state upon admission, informed consent  
249 was obtained from their legal guardian first, and Patient A also provided her own informed  
250 consent upon recovery. The wavelet analysis was performed using the *WaveletComp*  
251 package<sup>53</sup> in R version 4.2.0 (R Project for Statistical Computing) within Rstudio version  
252 1.4.1106 (Rstudio).

253 **3. Results**

254 **3.1 Validation of uTEV and uADEVs**

255 **Figure 1 (a–h)** shows the isolation schematic diagram of uADEVs and their validation  
256 using NTA, TEM, and western blotting. NTA confirmed that the EV diameters were within  
257 the expected size range for small EVs. TEM images revealed characteristic EV-like structures  
258 in both uTEV and uADEV samples. Western blotting showed positive expression of three EV  
259 markers (CD63, CD9, and Alix) in both uTEV and uADEV samples. Additionally, uADEVs  
260 exhibited positive expression of an astrocyte marker (GFAP). Notably, two kidney markers,  
261 NCC2 and NKCC, were detected in the uTEV sample but not in the uADEVs samples. See  
262 **Supplementary Material 1 (sFigure 1)** for the original western blotting images.

263

264 **3.2 Comparisons between uTEVs and uADEVs**

265 Particle concentrations in uADEVs ( $5.3 \pm 1.6E10/ml$ ) were significantly lower compared  
266 to uTEVs ( $1.9 \pm 0.78E12/ml$ ). Given the sample volumes of uADEVs (216  $\mu$ l) and uTEVs  
267 (900  $\mu$ l), this indicates that uADEVs constitute about 0.81% of uTEVs. In contrast,  
268 neurotrophin levels in uADEVs were notably higher compared to uTEVs. To quantify the  
269 enhancement in astrocytic signal clarity within the CNS, we assessed the signal-to-noise ratio  
270 (SNR) by calculating the fold increase in neurotrophin concentrations. This analysis revealed  
271 a range of fold changes between 23.1 and 88.1 across seven neurotrophins, as detailed in  
272 **Figure 1(i)** and **Table 1**.

273

274

275 **Table 1. Fold changes of uADEVs to uTEVs.**

Variable	In uADEV (pg) <sup>a</sup>	In uTEV (pg) <sup>a</sup>	Increased Fold Change		<i>P</i>
	Mean ± SD	Mean ± SD	Mean ± SD	Median [IQR]	
BDNF	0.625 ± 0.246	0.010 ± 0.005	88.1 ± 69.3	61.0 [33.8; 112.1]	<0.001
EGF	38.153 ± 9.364	2.761 ± 2.126	23.1 ± 18.1	17.6 [8.3; 32.6]	<0.001
FGF-2	3.747 ± 1.991	0.162 ± 0.124	28.8 ± 16.5	29.9 [19.9; 30.6]	0.001
GDNF	23.355 ± 4.966	0.897 ± 0.685	32.8 ± 11.4	31.0 [28.8; 44.0]	<0.001
GFAP	7.826 ± 6.890	0.285 ± 0.203	29.9 ± 17.3	29.0 [15.0; 33.6]	0.011
NGF-β	0.985 ± 0.879	0.041 ± 0.028	40.4 ± 47.5	13.0 [9.6; 80.7]	0.012
S100β	0.765 ± 0.219	0.029 ± 0.021	43.7 ± 34.6	35.4 [17.8; 59.9]	<0.001

276 Note: a: Normalized to every 10<sup>10</sup> particles.

277

### 278 **3.2 Case: the longitudinal trajectory of proteins in uADEVs in an encephalitis patient**

279 **Figure 2** demonstrated the comprehensive dynamic picture of Patient A during  
280 hospitalization.

281

### 282 **3.3 Data availability**

283 All data were presented in the **Supplementary Material 2: Individual Participant**

284 **Data.**

285

286

#### 287 4. Discussion

288 In this study, we established a method to extract ADEVs from urine, facilitating the  
289 tracing of *in vivo* specific molecular signal in the CNS. Then, as a demonstration, we tracked  
290 the trajectory of NMDAR subunit GluN1 in uADEVs from a patient with anti-NMDAR  
291 encephalitis and employed wavelet analysis to identify significant components in the  
292 trajectory. This uADEVs protocol may offer a novel, non-invasive method for daily CNS  
293 monitoring, providing a valuable tool for biomarker discovery and etiological studies of  
294 rapidly evolving CNS diseases.

295 In order to verify the isolation efficiency of uADEVs, we compared the neurotrophin  
296 concentrations normalized to particle numbers in uTEV and uADEV samples. Mean fold  
297 changes ranged from 23.1 (EGF) to 88.1 (BDNF) (**Figure 1(i)**). This enrichment can be  
298 interpreted from the signal-theoretic perspective as an improvement in the SNR of  
299 astrocyte-derived signals in uTEVs.

300 To illustrate the concept of signal amplification, we consider a scenario where “a”  
301 represents the total number of EVs extracted from a urine sample, and “b” represents the  
302 number of EVs are derived from astrocytes (uADEVs). The original SNR of the signal from  
303 astrocytes in uTEVs is  $\frac{b}{a}$ , and the SNR of the same signal in uADEVs is  $\frac{b}{b} = 1$ . Therefore,  
304 the amplification factor is  $\frac{1}{\frac{b}{a}} = \frac{a}{b}$ , which is approximately 123 based on particle number ratio  
305 in this present study. This indicates that the SNR of a signal from astrocytes in uGLAST<sup>+</sup>EVs  
306 is 123 times higher than in uTEVs, representing an upper bound for the increase in SNR. The  
307 increase in SNR was also assessed using astrocyte-related molecules, such as neurotrophins.  
308 The fold increase in the ratio of their concentration to particle number in uADEV samples

309 compared to uTEV samples provides an estimate of the lower bound of SNR enhancement.  
310 The results revealed a maximum 88-fold increase (BDNF), which is slightly lower than the  
311 estimate based on particle count. Our approach, therefore, leads to an approximately  
312 88–123-fold increase in SNR for signals from astrocytes via uADEVs. Nevertheless, these are  
313 preliminary estimates, and further studies are warranted to refine these calculations.

314 Another key issue of this protocol is to estimate potential contamination mainly from  
315 urogenital tract. Hence, we selected two widely used markers of uTEVs (NKCC2 and NCC)  
316 in urinary EV studies<sup>31,54</sup>. Western blotting results showed that these two markers were highly  
317 expressed in uTEV samples as expected, but were barely detected in uADEV samples (**Figure**  
318 **1(h)**). These results indicate minimal kidney-derived contamination in uADEVs. Along with  
319 evidence of neurotrophins, we established that the majority of these uGLAST<sup>+</sup>EVs were  
320 ADEVs.

321 Theoretically, uTEVs may also contain EVs derived from other CNS cells, such as  
322 neurons and various types of glial cells, including microglia and oligodendrocytes, which  
323 could be isolated using similar methods. For other types of BDEVs, such as NDEVs, L1 cell  
324 adhesion molecule (L1CAM) is commonly used as a marker<sup>55-57</sup>. However, L1CAM  
325 expression is also detected in the kidney<sup>58</sup>, potentially compromising the purity of urinary  
326 L1CAM<sup>+</sup>EVs that are truly derived from CNS. Given that GLAST is believed to be  
327 predominantly expressed in astrocytes, we selected urinary GLAST<sup>+</sup>EV/ADEV as an initial  
328 proof-of-concept for isolating BDEVs from urine. We are developing appropriate  
329 methodologies to exclude the interference of EVs from the urological system, enabling the  
330 enrichment of other types of BDEVs from urine.

331 UC has been extensively used for uTEV enrichment for decades, with a common  
332 protocol involving UC at 100,000 g for 70 minutes, repeated twice, to isolate uTEVs<sup>59-65</sup>.  
333 Investigations indicated that extended centrifugation, potentially up to four hours, may  
334 enhance EV yields<sup>66</sup>. In our study, given the low proportion of uADEVs in uTEVs, our  
335 primary objective was to increase the yield of uTEVs rather than focusing on purity at the  
336 first stage. Therefore, we conducted a pilot study to refine UC parameters for optimal uTEVs  
337 yield, detailed in **Supplementary Material 3 (The Determination of the Duration of**  
338 **Ultracentrifugation)**, and the TEM images (**Figure 1(c and d)**) suggested that the applied  
339 UC parameters (150,000 g for 150 minutes) did not significantly introduce impurities.

340 We also presented longitudinal data from a patient with anti-NMDAR encephalitis to  
341 showcase the potential of uADEVs in revealing *in vivo* molecular trajectories and  
342 demonstrate the application of signal processing algorithms for enhanced analysis (**Figure 2**).  
343 Anti-NMDAR encephalitis is a well-defined autoimmune disease characterized by  
344 autoantibodies targeting the NMDA receptor (primarily the GluN1 subunit) in the CNS<sup>67,68</sup>.  
345 The first-line immunosuppressive therapy typically comprising steroids, intravenous  
346 immunoglobulin, and plasma exchange, followed by second-line therapies including  
347 rituximab or methotrexate/cyclophosphamide, alone or in combination<sup>69,70</sup>. In this  
348 longitudinal data, we observed dynamic changes in GluN1 within uADEVs. To analyze these  
349 dynamic changes, we applied wavelet analysis, a widely used algorithm that decomposes  
350 complex signals into simpler components<sup>71</sup>. This approach enables us to identify and  
351 characterize the underlying patterns in GluN1 fluctuations. We discovered that it consists of  
352 two main significant components, with the shorter periodic component (approximately 6–8

353 days) shown in **Figure 2(h)** and the longer one (approximately 32 days) in **Figure 2(i)**. Based  
354 on prior knowledge, here we made some guesses. Since some EVs are formed through cell  
355 membrane invagination, and inevitably carry extracellular molecules<sup>72-74</sup>. Additionally, the  
356 shape and time course of this component resemble the trajectory of GluN1 in CSF (**Figure**  
357 **2(e)**), we speculate that the longer-period component may reflect the changes in extracellular  
358 GluN1 levels. The shape and timing of the shorter period component appeared to correlate  
359 with the treatment. Following the combination of methotrexate and rituximab, the trajectory  
360 of the short-period component increased. Considering the plasma membrane origin of EV  
361 membranes and previous reports of NMDAR density reduction in anti-NMDAR encephalitis  
362 patients and its restoration upon effective treatment<sup>75</sup>, we hypothesize that this short-period  
363 signal may reflected the dynamic response of NMDAR density on astrocyte plasma  
364 membranes to treatment. However, it is important to note that definitive conclusions cannot  
365 be drawn from a single case in this study, the aforementioned conjectures are more suitable as  
366 new hypotheses for further investigation. Our study suggests that by increasing the number  
367 and density of sampling points, sophisticated powerful signal processing algorithms like  
368 wavelet analysis could be applied to extract meaningful information from these dynamic CNS  
369 *in vivo* signals, enabling the formulation of more specific hypotheses for targeted  
370 experimental validation.

371

## 372 **Significance**

373 The temporal depth provided by uADEVs may hold significant promise for the  
374 discovery of novel biomarkers for CNS diseases, particularly those that progress rapidly. One

375 prerequisite for a molecule (or a combination of molecules) to become a reliable diagnostic  
376 marker, is that it must be “individual-level” identifiable. Nevertheless, for rapidly evolving  
377 CNS diseases, conventional follow-up frequencies (monthly, semiannually, or annually) may  
378 not be sufficient to capture the dynamic molecular changes associated with disease  
379 progression, according to the Nyquist-Shannon sampling theorem<sup>15</sup> (**Figure 3(a)**). However,  
380 our uADEVs protocol could offer a non-invasive solution with the potential for sampling up  
381 to daily. With advancements in detection technology and reduced urine volume requirements,  
382 hourly sampling may become feasible, enabling the capture of CNS dynamics at an  
383 unprecedented level. In short, uADEVs allow us to capture *in vivo* molecular “movies” of the  
384 CNS at the individual level, rather than capturing static “snapshots”. This further implies that,  
385 diagnosing a disease with distinct episodes may require multiple longitudinal tests, even  
386 including artificial perturbations (analogous to an oral glucose tolerance test). This is because  
387 a single-time biomarker test may not be sufficient to capture the dynamic nature of such  
388 diseases.

389       Even if no new biomarkers are discovered, uADEVs will facilitate the falsification of  
390 potential hypotheses. As illustrated in **Figure 3(b)**, if the trajectory of a candidate molecule  
391 aligns with, but lags behind, the symptom trajectory, it can be inferred that it is not the cause  
392 but rather a consequence or a confounding factor. Conversely, only candidate molecules with  
393 trajectories preceding the symptom trajectory are likely to be causal. Naturally, things become  
394 somewhat simpler when we can precisely trace the molecular trajectories at the  
395 individual-level.

396       Identifying reliable biomarkers for rapidly changing CNS disorders, such as depression,

397 is challenging, potentially due to their high heterogeneity, and the fluctuating molecular  
398 signals themselves might also contribute to this heterogeneity. As illustrated in **Figure 3(c)**,  
399 even assuming all patients with a specific disease share identical molecular trajectories (this  
400 assumption is inaccurate but serves to demonstrate the concept), heterogeneity can also arise  
401 from different sampling points along the trajectory. This time-induced heterogeneity could be  
402 a significant factor. However, with adequate sampling frequency, we can capture individual  
403 molecular trajectories (**Figure 3(d)**). Various *post-hoc* algorithms, such as realigning  
404 trajectories based on their peaks, can then be employed to reduce time-induced heterogeneity  
405 (**Figure 3(e)**). While this is a simplified model, and heterogeneity manifests in various forms  
406 with greater complexity in real-world data, we believe that high-frequency sampling provides  
407 more opportunities for data processing using multiple algorithms, enabling deeper  
408 exploration.

409 This methodology may introduce a novel experimental paradigm, which we termed the  
410 “Time Machine of Sampling” (**Figure 3(f)**). Studying the recurrence of CNS diseases is often  
411 hampered by the limited availability of samples from the period preceding recurrence. These  
412 samples are crucial as they may contain the molecular trigger signals for recurrence.  
413 Fortunately, uADEVs can be non-invasively collected and directly reflect CNS signals. For  
414 CNS diseases with a high recurrence probability, we propose collecting and storing urine  
415 samples at a high frequency. When monitoring a patient for recurrence, we can unseal  
416 samples collected before the recurrence time point to extract uADEVs for analysis. This may  
417 enable the collection of samples with a sufficient sampling rate from the period preceding  
418 CNS disease recurrence. Hence, we term this paradigm the “Time Machine of Sampling” as it

419 allows us to go back in time and collect samples before recurrence. This paradigm may  
420 facilitate the identification of molecular triggers preceding disease recurrence.

421 Our study may also enhance therapeutic monitoring. Timely assessment of treatment  
422 efficacy is essential for precision medicine. As demonstrated in Patient A, the GluN1  
423 concentrations in uADEVs appear to be responsive to treatment. This suggests that the  
424 uADEVs approach could provide more rapid and timely feedback for diseases that demand  
425 close therapeutic monitoring. Further research in this area is warranted.

426 It is noteworthy that, based on the protocol's principle, it is theoretically possible to  
427 isolate not only ADEVs from the CNS but also EVs from other CNS cell types, organs, or  
428 tissues from uTEVs, if these cells express specific surface markers. We anticipate that urine  
429 samples may hold significant value for disease studies beyond CNS and urological disorders.

430

### 431 **Limitations**

432 First, alternative isolation protocols, such as size-exclusion chromatography (SEC), may  
433 be suitable for laboratories lacking ultracentrifuges. Additionally, UF may lead to a significant  
434 loss of uTEVs. Employing high-capacity ultrafiltration tubes to directly collect uTEVs  
435 without UF may potentially enhance the yield of uADEVs. However, due to laboratory  
436 constraints, we were unable to attempt this, and further investigation is required by external  
437 laboratories. Second, while the yield of uTEVs is substantial, the absolute number of  
438 uADEVs remains low, limiting multi-omics-based high-throughput assays. To address this  
439 challenge, we are endeavoring to develop methodologies for high-throughput studies utilizing  
440 minimal amounts of uADEVs. Third, the impact of subjects' disease status, particularly

441 urological diseases, on uADEVs remains unclear. Further research is needed to address this  
442 question. Fourth, the mechanism by which ADEVs traverse the glomerular basement  
443 membrane into urine remains unknown. Elucidating this mechanism may significantly  
444 enhance the utility of uADEVs. Fifth, this study utilized fresh urine samples. The applicability  
445 of frozen or concentrated urine samples after thawing remains undetermined. Future studies  
446 should investigate the effect of sample storage conditions on uADEVs. After all, compared  
447 with unconcentrated urine samples, storing concentrated urine samples could alleviate  
448 inventory pressure on biobanks.

449

## 450 **Conclusions**

451 In this study, we proposed a simple method for isolating urinary ADEVs, enabling  
452 non-invasive monitoring of CNS *in vivo* activity with high sampling rates, up to daily or even  
453 half-daily. This approach, analogous to capturing molecular “movies” of the brain, coupled  
454 with appropriate signal processing algorithms, holds promise for identifying novel biomarkers  
455 or illuminating the etiology of rapidly evolving CNS diseases by tracking the precise  
456 trajectories of target molecules.

457 **References**

- 458 1. Abi-Dargham A, Moeller SJ, Ali F, et al. Candidate biomarkers in psychiatric disorders:  
459 state of the field. *World Psychiatry*. 2023;22(2):236-262. doi:10.1002/wps.21078
- 460 2. García-Gutiérrez MS, Navarrete F, Sala F, Gasparyan A, Austrich-Olivares A,  
461 Manzanares J. Biomarkers in Psychiatry: Concept, Definition, Types and Relevance to  
462 the Clinical Reality. *Front Psychiatry*. 2020;11:432. doi:10.3389/fpsyt.2020.00432
- 463 3. Kadry H, Noorani B, Cucullo L. A blood-brain barrier overview on structure, function,  
464 impairment, and biomarkers of integrity. *Fluids Barriers CNS*. 2020;17(1):69.  
465 doi:10.1186/s12987-020-00230-3
- 466 4. Lerche S, Zimmermann M, Wurster I, et al. CSF and Serum Levels of Inflammatory  
467 Markers in PD: Sparse Correlation, Sex Differences and Association With  
468 Neurodegenerative Biomarkers. *Front Neurol*. 2022;13:834580.  
469 doi:10.3389/fneur.2022.834580
- 470 5. Beems T, Simons KS, Van Geel WJA, De Reus HPM, Vos PE, Verbeek MM. Serum- and  
471 CSF-concentrations of brain specific proteins in hydrocephalus. *Acta Neurochir (Wien)*.  
472 2003;145(1):37-43. doi:10.1007/s00701-002-1019-1
- 473 6. Wijeyekoon RS, Moore SF, Farrell K, Breen DP, Barker RA, Williams-Gray CH.  
474 Cerebrospinal Fluid Cytokines and Neurodegeneration-Associated Proteins in  
475 Parkinson's Disease. *Mov Disord*. 2020;35(6):1062-1066. doi:10.1002/mds.28015
- 476 7. Eidson LN, Kannarkat GT, Barnum CJ, et al. Candidate inflammatory biomarkers display

- 477 unique relationships with alpha-synuclein and correlate with measures of disease severity  
478 in subjects with Parkinson's disease. *J Neuroinflammation*. 2017;14(1):164.  
479 doi:10.1186/s12974-017-0935-1
- 480 8. Le Bastard N, Aerts L, Leurs J, Blomme W, De Deyn PP, Engelborghs S. No correlation  
481 between time-linked plasma and CSF Abeta levels. *Neurochem Int*. 2009;55(8):820-825.  
482 doi:10.1016/j.neuint.2009.08.006
- 483 9. Gigase FAJ, Smith E, Collins B, et al. The association between inflammatory markers in  
484 blood and cerebrospinal fluid: a systematic review and meta-analysis. *Mol Psychiatry*.  
485 2023;28(4):1502-1515. doi:10.1038/s41380-023-01976-6
- 486 10. Jack CR, Bennett DA, Blennow K, et al. NIA-AA Research Framework: Toward a  
487 biological definition of Alzheimer's disease. *Alzheimer's & Dementia*.  
488 2018;14(4):535-562. doi:10.1016/j.jalz.2018.02.018
- 489 11. Blessed G, Tomlinson BE, Roth M. The association between quantitative measures of  
490 dementia and of senile change in the cerebral grey matter of elderly subjects. *Br J*  
491 *Psychiatry*. 1968;114(512):797-811. doi:10.1192/bjp.114.512.797
- 492 12. Parnetti L, Gaetani L, Eusebi P, et al. CSF and blood biomarkers for Parkinson's disease.  
493 *Lancet Neurol*. 2019;18(6):573-586. doi:10.1016/S1474-4422(19)30024-9
- 494 13. Olsson B, Lautner R, Andreasson U, et al. CSF and blood biomarkers for the diagnosis of  
495 Alzheimer's disease: a systematic review and meta-analysis. *Lancet Neurol*.  
496 2016;15(7):673-684. doi:10.1016/S1474-4422(16)00070-3

- 497 14. Fayyad M, Salim S, Majbour N, et al. Parkinson's disease biomarkers based on  
498  $\alpha$ -synuclein. *J Neurochem*. 2019;150(5):626-636. doi:10.1111/jnc.14809
- 499 15. Shannon CE. Communication in the Presence of Noise. *Proceedings of the IRE*.  
500 1949;37(1):10-21. doi:10.1109/JRPROC.1949.232969
- 501 16. Théry C, Witwer KW, Aikawa E, et al. Minimal information for studies of extracellular  
502 vesicles 2018 (MISEV2018): a position statement of the International Society for  
503 Extracellular Vesicles and update of the MISEV2014 guidelines. *J Extracell Vesicles*.  
504 2018;7(1):1535750. doi:10.1080/20013078.2018.1535750
- 505 17. Liang Y, Lehrich BM, Zheng S, Lu M. Emerging methods in biomarker identification for  
506 extracellular vesicle-based liquid biopsy. *J Extracell Vesicles*. 2021;10(7):e12090.  
507 doi:10.1002/jev2.12090
- 508 18. Ramos-Zaldívar HM, Polakovicova I, Salas-Huenuleo E, et al. Extracellular vesicles  
509 through the blood-brain barrier: a review. *Fluids Barriers CNS*. 2022;19(1):60.  
510 doi:10.1186/s12987-022-00359-3
- 511 19. Shi M, Sheng L, Stewart T, Zabetian CP, Zhang J. New windows into the brain: Central  
512 nervous system-derived extracellular vesicles in blood. *Prog Neurobiol*. 2019;175:96-106.  
513 doi:10.1016/j.pneurobio.2019.01.005
- 514 20. Jia L, Qiu Q, Zhang H, et al. Concordance between the assessment of A $\beta$ 42, T-tau, and  
515 P-T181-tau in peripheral blood neuronal-derived exosomes and cerebrospinal fluid.  
516 *Alzheimer's & Dementia*. 2019;15(8):1071-1080. doi:10.1016/j.jalz.2019.05.002

- 517 21. Jia L, Zhu M, Kong C, et al. Blood neuro-exosomal synaptic proteins predict Alzheimer's  
518 disease at the asymptomatic stage. *Alzheimers Dement.* 2021;17(1):49-60.  
519 doi:10.1002/alz.12166
- 520 22. Agliardi C, Meloni M, Guerini FR, et al. Oligomeric  $\alpha$ -Syn and SNARE complex  
521 proteins in peripheral extracellular vesicles of neural origin are biomarkers for  
522 Parkinson's disease. *Neurobiol Dis.* 2021;148:105185. doi:10.1016/j.nbd.2020.105185
- 523 23. Dutta S, Hornung S, Kruayatidee A, et al.  $\alpha$ -Synuclein in blood exosomes  
524 immunoprecipitated using neuronal and oligodendroglial markers distinguishes  
525 Parkinson's disease from multiple system atrophy. *Acta Neuropathol.*  
526 2021;142(3):495-511. doi:10.1007/s00401-021-02324-0
- 527 24. Si X, Tian J, Chen Y, Yan Y, Pu J, Zhang B. Central Nervous System-Derived Exosomal  
528 Alpha-Synuclein in Serum May Be a Biomarker in Parkinson's Disease. *Neuroscience.*  
529 2019;413:308-316. doi:10.1016/j.neuroscience.2019.05.015
- 530 25. Stuenkel A, Kraus T, Chatterjee M, et al.  $\alpha$ -Synuclein in Plasma-Derived Extracellular  
531 Vesicles Is a Potential Biomarker of Parkinson's Disease. *Mov Disord.*  
532 2021;36(11):2508-2518. doi:10.1002/mds.28639
- 533 26. Zou J, Guo Y, Wei L, Yu F, Yu B, Xu A. Long Noncoding RNA POU3F3 and  $\alpha$ -Synuclein  
534 in Plasma L1CAM Exosomes Combined with  $\beta$ -Glucocerebrosidase Activity: Potential  
535 Predictors of Parkinson's Disease. *Neurotherapeutics.* 2020;17(3):1104-1119.  
536 doi:10.1007/s13311-020-00842-5

- 537 27. Jiang C, Hopfner F, Berg D, et al. Validation of  $\alpha$ -Synuclein in  
538 L1CAM-Immunocaptured Exosomes as a Biomarker for the Stratification of  
539 Parkinsonian Syndromes. *Movement Disord*. Published online April 7, 2021:mds.28591.  
540 doi:10.1002/mds.28591
- 541 28. Delgado-Peraza F, Noguera-Ortiz CJ, Volpert O, et al. Neuronal and Astrocytic  
542 Extracellular Vesicle Biomarkers in Blood Reflect Brain Pathology in Mouse Models of  
543 Alzheimer's Disease. *Cells-basel*. 2021;10(5):993. doi:10.3390/cells10050993
- 544 29. Cheng L, Vella LJ, Barnham KJ, McLean C, Masters CL, Hill AF. Small RNA  
545 fingerprinting of Alzheimer's disease frontal cortex extracellular vesicles and their  
546 comparison with peripheral extracellular vesicles. *J Extracell Vesicles*.  
547 2020;9(1):1766822. doi:10.1080/20013078.2020.1766822
- 548 30. Huang Y, Driedonks TAP, Cheng L, et al. Brain Tissue-Derived Extracellular Vesicles in  
549 Alzheimer's Disease Display Altered Key Protein Levels Including Cell Type-Specific  
550 Markers. *J Alzheimers Dis*. 2022;90(3):1057-1072. doi:10.3233/JAD-220322
- 551 31. Merchant ML, Rood IM, Deegens JKJ, Klein JB. Isolation and characterization of urinary  
552 extracellular vesicles: implications for biomarker discovery. *Nat Rev Nephrol*.  
553 2017;13(12):731-749. doi:10.1038/nrneph.2017.148
- 554 32. Fraser KB, Rawlins AB, Clark RG, et al. Ser(P)-1292 LRRK2 in urinary exosomes is  
555 elevated in idiopathic Parkinson's disease. *Mov Disord*. 2016;31(10):1543-1550.  
556 doi:10.1002/mds.26686

- 557 33. Harpole M, Davis J, Espina V. Current state of the art for enhancing urine biomarker  
558 discovery. *Expert Rev Proteomics*. 2016;13(6):609-626.  
559 doi:10.1080/14789450.2016.1190651
- 560 34. Svenningsen P, Sabaratnam R, Jensen BL. Urinary extracellular vesicles: Origin, role as  
561 intercellular messengers and biomarkers; efficient sorting and potential treatment options.  
562 *Acta Physiol (Oxf)*. 2020;228(1):e13346. doi:10.1111/apha.13346
- 563 35. Wang Z, Hill S, Luther JM, Hachey DL, Schey KL. Proteomic analysis of urine  
564 exosomes by multidimensional protein identification technology (MudPIT). *Proteomics*.  
565 2012;12(2):329-338. doi:10.1002/pmic.201100477
- 566 36. Zhu Q, Cheng L, Deng C, et al. The genetic source tracking of human urinary exosomes.  
567 *Proc Natl Acad Sci U S A*. 2021;118(43):e2108876118. doi:10.1073/pnas.2108876118
- 568 37. Kang M, Jordan V, Blenkiron C, Chamley LW. Biodistribution of extracellular vesicles  
569 following administration into animals: A systematic review. *J Extracell Vesicles*.  
570 2021;10(8):e12085. doi:10.1002/jev2.12085
- 571 38. Iannotta D, A A, Kijas AW, Rowan AE, Wolfram J. Entry and exit of extracellular vesicles  
572 to and from the blood circulation. *Nat Nanotechnol*. Published online December 18, 2023.  
573 doi:10.1038/s41565-023-01522-z
- 574 39. Cheng Y, Wang X, Yang J, et al. A translational study of urine miRNAs in acute  
575 myocardial infarction. *J Mol Cell Cardiol*. 2012;53(5):668-676.  
576 doi:10.1016/j.jmcc.2012.08.010

- 577 40. Chen Y, Xia K, Chen L, Fan D. Increased Interleukin-6 Levels in the Astrocyte-Derived  
578 Exosomes of Sporadic Amyotrophic Lateral Sclerosis Patients. *Front Neurosci-switz*.  
579 2019;13:574. doi:10.3389/fnins.2019.00574
- 580 41. Goetzl EJ, Mustapic M, Kapogiannis D, et al. Cargo proteins of plasma astrocyte-derived  
581 exosomes in Alzheimer's disease. *The FASEB Journal*. 2016;30(11):3853-3859.  
582 doi:10.1096/fj.201600756R
- 583 42. Goetzl EJ, Schwartz JB, Abner EL, Jicha GA, Kapogiannis D. High complement levels in  
584 astrocyte-derived exosomes of Alzheimer disease. *Ann Neurol*. 2018;83(3):544-552.  
585 doi:10.1002/ana.25172
- 586 43. Goetzl EJ, Srihari VH, Guloksuz S, Ferrara M, Tek C, Heninger GR. Decreased  
587 mitochondrial electron transport proteins and increased complement mediators in plasma  
588 neural-derived exosomes of early psychosis. *Transl Psychiatry*. 2020;10(1):361.  
589 doi:10.1038/s41398-020-01046-3
- 590 44. Goetzl EJ, Yaffe K, Peltz CB, et al. Traumatic brain injury increases plasma  
591 astrocyte-derived exosome levels of neurotoxic complement proteins. *FASEB J*.  
592 2020;34(2):3359-3366. doi:10.1096/fj.201902842R
- 593 45. Lee EE, Winston-Gray C, Barlow JW, Rissman RA, Jeste DV. Plasma Levels of Neuron-  
594 and Astrocyte-Derived Exosomal Amyloid Beta1-42, Amyloid Beta1-40, and  
595 Phosphorylated Tau Levels in Schizophrenia Patients and Non-psychiatric Comparison  
596 Subjects: Relationships With Cognitive Functioning and Psychopathology. *Front*

- 597        *Psychiatry*. 2020;11:532624. doi:10.3389/fpsyt.2020.532624
- 598    46. Winston CN, Goetzl EJ, Schwartz JB, Elahi FM, Rissman RA. Complement protein  
599        levels in plasma astrocyte-derived exosomes are abnormal in conversion from mild  
600        cognitive impairment to Alzheimer's disease dementia. *Alzheimers Dement (Amst)*.  
601        2019;11:61-66. doi:10.1016/j.dadm.2018.11.002
- 602    47. Xie XH, Lai WT, Xu SX, et al. Hyper-inflammation of Astrocytes in Patients of Major  
603        Depressive Disorder: Evidence from Serum Astrocyte-derived Extracellular Vesicles.  
604        *Brain Behav Immun*. Published online December 29, 2022:S0889-1591(22)00472-X.  
605        doi:10.1016/j.bbi.2022.12.014
- 606    48. World Medical Association. World Medical Association Declaration of Helsinki: ethical  
607        principles for medical research involving human subjects. *JAMA*.  
608        2013;310(20):2191-2194. doi:10.1001/jama.2013.281053
- 609    49. Xu SX, Xie XH, Yao L, et al. Human in vivo evidence of reduced astrocyte activation and  
610        neuroinflammation in patients with treatment-resistant depression following  
611        electroconvulsive therapy. *Psychiatry Clin Neurosci*. 2023;77(12):653-664.  
612        doi:10.1111/pcn.13596
- 613    50. Tamm I, Horsfall FL. A mucoprotein derived from human urine which reacts with  
614        influenza, mumps, and Newcastle disease viruses. *J Exp Med*. 1952;95(1):71-97.  
615        doi:10.1084/jem.95.1.71
- 616    51. Kosanović M, Janković M. Isolation of urinary extracellular vesicles from Tamm-

- 617        Horsfall protein-depleted urine and their application in the development of a  
618        lectin-exosome-binding        assay.        *Biotechniques*.        2014;57(3):143-149.  
619        doi:10.2144/000114208
- 620    52. Xu SX, Xie XH, Yao L, et al. Human in vivo evidence of reduced astrocyte activation and  
621        neuroinflammation in patients with treatment-resistant depression following  
622        electroconvulsive therapy. *Psychiatry Clin Neurosci*. Published online September 7, 2023.  
623        doi:10.1111/pcn.13596
- 624    53. Roesch A, Schmidbauer H. WaveletComp: computational wavelet analysis. *R package*  
625        *version*. 2018;1(1).
- 626    54. Erdbrügger U, Blijdorp CJ, Bijnsdorp IV, et al. Urinary extracellular vesicles: A position  
627        paper by the Urine Task Force of the International Society for Extracellular Vesicles. *J*  
628        *Extracell Vesicles*. 2021;10(7):e12093. doi:10.1002/jev2.12093
- 629    55. Eren E, Leoutsakos JM, Troncoso J, Lyketsos CG, Oh ES, Kapogiannis D.  
630        Neuronal-Derived EV Biomarkers Track Cognitive Decline in Alzheimer’s Disease. *Cells*.  
631        2022;11(3):436. doi:10.3390/cells11030436
- 632    56. Saeedi S, Nagy C, Ibrahim P, et al. Neuron-derived extracellular vesicles enriched from  
633        plasma show altered size and miRNA cargo as a function of antidepressant drug response.  
634        *Mol Psychiatr*. 2021;26(12):7417-7424. doi:10.1038/s41380-021-01255-2
- 635    57. Goetzl EJ, Srihari VH, Mustapic M, Kapogiannis D, Heninger GR. Abnormal levels of  
636        mitochondrial Ca<sup>2+</sup> channel proteins in plasma neuron-derived extracellular vesicles of

- 637 early schizophrenia. *FASEB J.* 2022;36(8):e22466. doi:10.1096/fj.202200792RR
- 638 58. Allory Y, Audard V, Fontanges P, Ronco P, Debiec H. The L1 cell adhesion molecule is a  
639 potential biomarker of human distal nephron injury in acute tubular necrosis. *Kidney Int.*  
640 2008;73(6):751-758. doi:10.1038/sj.ki.5002640
- 641 59. Zhao Y, Wang Y, Zhao E, et al. PTRF/CAVIN1, regulated by SHC1 through the EGFR  
642 pathway, is found in urine exosomes as a potential biomarker of ccRCC. *Carcinogenesis.*  
643 2020;41(3):274-283. doi:10.1093/carcin/bgz147
- 644 60. Ramirez-Garrastacho M, Berge V, Linē A, Llorente A. Potential of miRNAs in urinary  
645 extracellular vesicles for management of active surveillance in prostate cancer patients.  
646 *Br J Cancer.* 2022;126(3):492-501. doi:10.1038/s41416-021-01598-1
- 647 61. Lapitz A, Arbelaiz A, O'Rourke CJ, et al. Patients with Cholangiocarcinoma Present  
648 Specific RNA Profiles in Serum and Urine Extracellular Vesicles Mirroring the Tumor  
649 Expression: Novel Liquid Biopsy Biomarkers for Disease Diagnosis. *Cells.*  
650 2020;9(3):721. doi:10.3390/cells9030721
- 651 62. Olivares D, Perez-Hernandez J, Perez-Gil D, Chaves FJ, Redon J, Cortes R. Optimization  
652 of small RNA library preparation protocol from human urinary exosomes. *J Transl Med.*  
653 2020;18(1):132. doi:10.1186/s12967-020-02298-9
- 654 63. Skotland T, Ekroos K, Kauhanen D, et al. Molecular lipid species in urinary exosomes as  
655 potential prostate cancer biomarkers. *Eur J Cancer.* 2017;70:122-132.  
656 doi:10.1016/j.ejca.2016.10.011

- 657 64. Øverbye A, Skotland T, Koehler CJ, et al. Identification of prostate cancer biomarkers in  
658 urinary exosomes. *Oncotarget*. 2015;6(30):30357-30376. doi:10.18632/oncotarget.4851
- 659 65. Zhu Q, Li Q, Niu X, et al. Extracellular Vesicles Secreted by Human Urine-Derived Stem  
660 Cells Promote Ischemia Repair in a Mouse Model of Hind-Limb Ischemia. *Cell Physiol*  
661 *Biochem*. 2018;47(3):1181-1192. doi:10.1159/000490214
- 662 66. Cvjetkovic A, Lötvall J, Lässer C. The influence of rotor type and centrifugation time on  
663 the yield and purity of extracellular vesicles. *J Extracell Vesicles*. 2014;3.  
664 doi:10.3402/jev.v3.23111
- 665 67. Graus F, Titulaer MJ, Balu R, et al. A clinical approach to diagnosis of autoimmune  
666 encephalitis. *Lancet Neurol*. 2016;15(4):391-404. doi:10.1016/S1474-4422(15)00401-9
- 667 68. Dalmau J, Armangué T, Planagumà J, et al. An update on anti-NMDA receptor  
668 encephalitis for neurologists and psychiatrists: mechanisms and models. *Lancet Neurol*.  
669 2019;18(11):1045-1057. doi:10.1016/S1474-4422(19)30244-3
- 670 69. Dalmau J, Lancaster E, Martinez-Hernandez E, Rosenfeld MR, Balice-Gordon R.  
671 Clinical experience and laboratory investigations in patients with anti-NMDAR  
672 encephalitis. *Lancet Neurol*. 2011;10(1):63-74. doi:10.1016/S1474-4422(10)70253-2
- 673 70. Martinez-Hernandez E, Horvath J, Shiloh-Malawsky Y, Sangha N, Martinez-Lage M,  
674 Dalmau J. Analysis of complement and plasma cells in the brain of patients with  
675 anti-NMDAR encephalitis. *Neurology*. 2011;77(6):589-593.  
676 doi:10.1212/WNL.0b013e318228c136

677 71. Torrence C, Compo GP. A Practical Guide to Wavelet Analysis. *Bull Amer Meteor Soc.*

678 1998;79(1):61-78. doi:10.1175/1520-0477(1998)079<0061:APGTWA>2.0.CO;2

679 72. Raposo G, Stoorvogel W. Extracellular vesicles: exosomes, microvesicles, and friends. *J*

680 *Cell Biol.* 2013;200(4):373-383. doi:10.1083/jcb.201211138

681 73. Grange C, Bussolati B. Extracellular vesicles in kidney disease. *Nat Rev Nephrol.*

682 2022;18(8):499-513. doi:10.1038/s41581-022-00586-9

683 74. Juan T, Fürthauer M. Biogenesis and function of ESCRT-dependent extracellular vesicles.

684 *Semin Cell Dev Biol.* 2018;74:66-77. doi:10.1016/j.semcdb.2017.08.022

685 75. Galovic M, Al-Diwani A, Vivekananda U, et al. In Vivo N-Methyl-d-Aspartate Receptor

686 (NMDAR) Density as Assessed Using Positron Emission Tomography During Recovery

687 From NMDAR-Antibody Encephalitis. *JAMA Neurol.* 2023;80(2):211-213.

688 doi:10.1001/jamaneurol.2022.4352

689

690

691 **Figure legends**

692 **Figure 1. Isolation and Validations of uADEVs.** (a) Schematic diagram of the uADEVs  
693 isolation protocol. (b and e) NTA results of uTEVs and uADEVs. (c, d, f, and g) TEM images  
694 of uTEVs and uADEVs (scale bars: 0.5  $\mu\text{m}$  and 100 nm). (h) Results of western blotting:  
695 Three EV markers (CD63, CD9 and Alix) and an astrocyte marker (GFAP) were present in  
696 the ADEVs sample, while two kidney markers (NKCC2 and NCC) were absent. (i)  
697 Significantly increased astrocyte-related neurotrophic factors in uADEVs.)

698

699 **Figure 2. Comprehensive dynamic picture of Patient A with anti-NMDAR encephalitis**

700 **during her hospitalization.** The x-axis in all panels marks the days since admission (Day 0 =  
701 admission day). Main treatment included an initial phase of four intravenous infusions of  
702 human  $\gamma$ -globulin (dose 25 g, indicated by 4 vertical dot-dash red lines). Simultaneously,  
703 glucocorticoid therapy was administered (represented by the green horizontal line above each  
704 subfigure, with the line's width indicating the equivalent dose of methylprednisolone).  
705 Additionally, intrathecal methotrexate administration (dose 10 mg, represented by vertical  
706 solid yellow lines) and rituximab therapy (dose 100 mg, indicated by vertical long-dash blue  
707 lines) were administered. Clinical symptoms were assessed using two scales: (a) the Glasgow  
708 Coma Scale (GCS) and (b) the modified Rankin Scale (mRS), showing gradual improvement  
709 following treatment. Given the use of the immunotherapy, we measured the (c) percentage of  
710 CD19+ cells in the blood, assessed via flow cytometry, dropped to nearly non-existent levels  
711 by Day 10. We also monitored NMDAR-antigen (Ag) titres in the CSF. (d) A decrease in  
712 NMDAR-Ag titers in the CSF was observed as the treatment progressed. Given that

713 anti-NMDA encephalitis is characterized by the presence of autoantibodies mainly against the  
714 NMDAR GluN1 subunit, leading to NMDARs damage through internalization, shedding, and  
715 extracellular release, we also measured (e) The concentrations of GluN1 in CSF. As  
716 NMDARs are also present on the surface of astrocytes, we simultaneously measured the (f)  
717 concentrations of GluN1 in uADEVs (pg/per 1E+10 particles). As the trajectory of GluN1 in  
718 uADEVs was also a dynamic signal, composed of various wave components. Therefore, we  
719 conducted wavelet analysis using the Morlet wavelet as mother wavelet to identify and  
720 separate the significant components of this dynamic signal. (g) Wavelet analysis results of the  
721  $\log(10)$  GluN1 trajectory in uADEVs are presented, with colors representing power, black  
722 lines indicating the highest peak (ridge) in the respective region, and white areas representing  
723 significant components. Two significant components were identified, one with a short period  
724 (approximately 6-8 days) located below and another with a period of over 20 (the strongest  
725 ridge is at approximately 32 days). These two significant components were then reconstructed  
726 as follows: (h) The trajectory of the reconstructed significant short-period component (red  
727 line), and (i) the long-period component (approximately 32 days, the blue line). The gray  
728 dashed line in (h) and (i) represent the original  $\log(10)$  trajectory (grey dashed lines).

729

730 **Figure 3. The Significance of the uADEV approach.** (a) The advantage of high-frequent  
731 sampling. (b) The detailed trajectories of target molecules may benefit for the exploration  
732 (Molecule A and B) and falsification (Molecule C) of pathological hypotheses. (c–e) Even  
733 under the assumption that all patients have the same molecular trajectories, yet, time-induced  
734 heterogeneity exist merely due to different sampling points along the trajectory. However,

735 individual-level detailed trajectories may allow some *post-hoc* algorithms, such as peak-based  
736 realignment, to reduce the time-induced heterogeneity. (f) The schematic diagram of the  
737 “Time Machine of Sampling”: for CNS diseases with a high probability of recurrence, we  
738 could collect urine samples at a high frequency and store them. When a patient is monitored  
739 for a recurrence, we could then unseal the samples before the recurrence time point (red  
740 arrows) to extract uADEVs to explore the reason of recurrence, like the “Time Machine”.  
741

742 **Supplementary Materials**

743 **Supplementary Material 1: sFigure 1. The original whole piece pictures of western**

744 **blotting.** GFAP: Anti-GFAP antibody (Abcam, Cat No: ab68428) at 1/5000 dilution, protein

745 loading amount: 13.7 µg Per lane. NKCC2: Anti-NKCC2 antibody (Abcam, Cat No:

746 ab171747) at 1/2000 dilution, protein loading amount: 4 µg per lane. NCC: Anti-NCC

747 antibody (Abcam, Cat No: ab95302) at 1/1000 dilution, protein loading amount: 1.5 µg per

748 lane. CD63: Anti-CD63 antibody (Abcam, Cat No: ab134045) at 1/700 dilution, protein

749 loading amount: 4.0 µg per lane. CD9: Anti-CD9 antibody (Abcam, Cat No: ab263019) at

750 1/700 dilution, protein loading amount: 5.7 µg per lane. Alix: Anti-Alix antibody (proteintech,

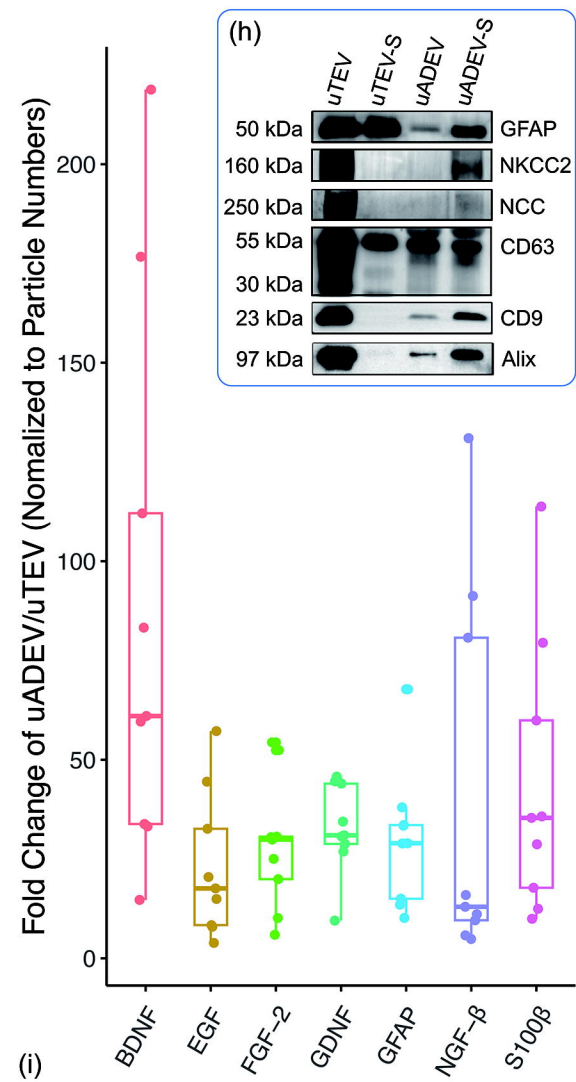
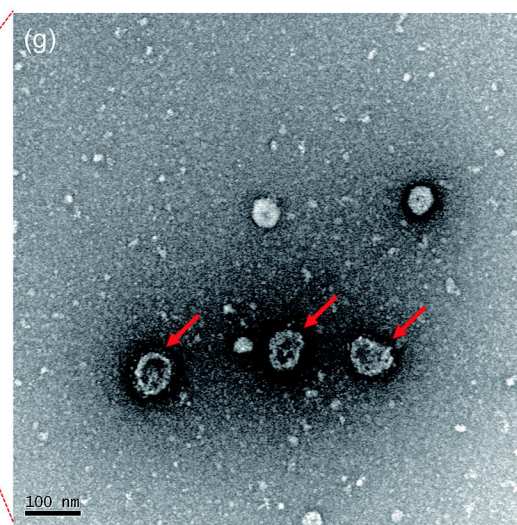
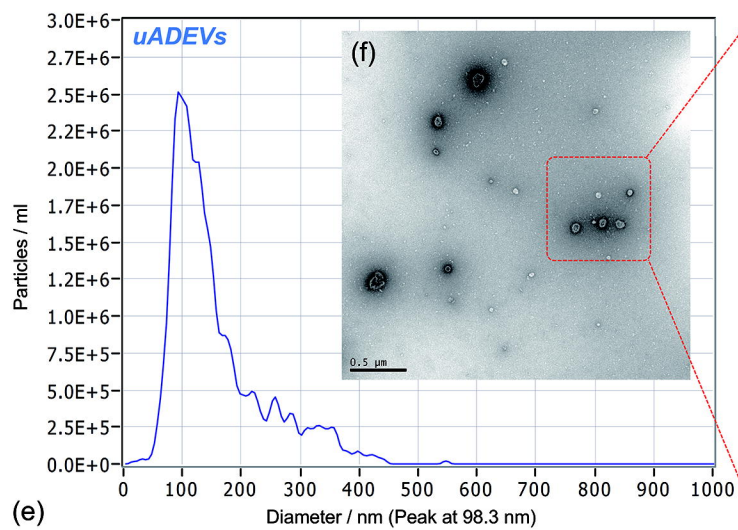
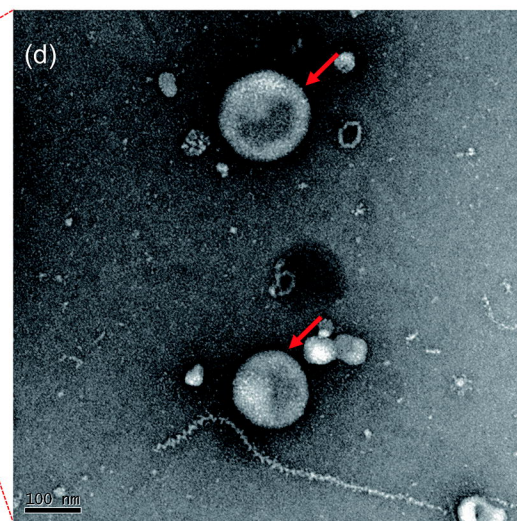
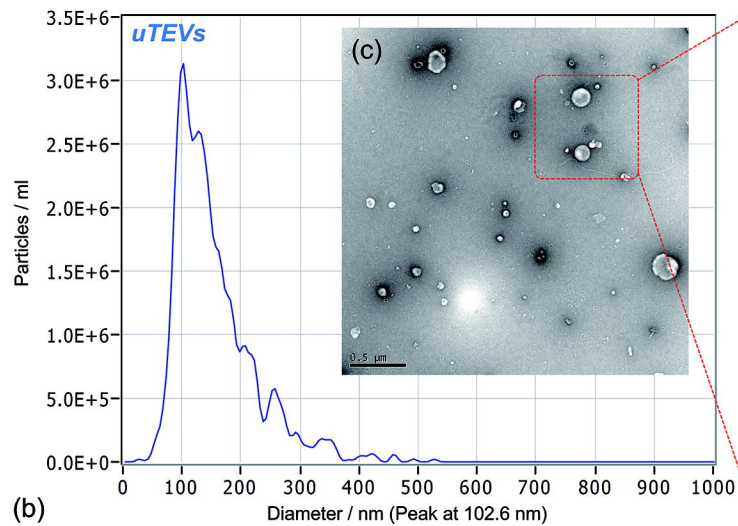
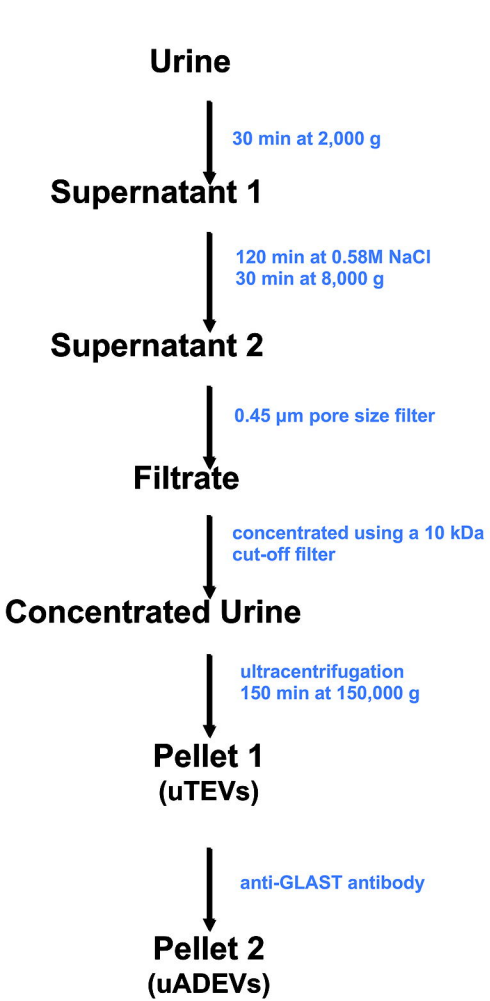
751 Cat No: 67715-1-Ig) at 1/2000 dilution, protein loading amount: 5.7 µg per lane.

752

753 **Supplementary Material 2: Individual Participant Data.**

754

755 **Supplementary Material 3: The Determination of the Duration of Ultracentrifugation.**



(a)

(i)

